Journal of Environmental Chemical Engineering 9 (2021) 106542

Contents lists available at ScienceDirect

Journal of Environmental Chemical Engineering

journal homepage: www.elsevier.com/locate/jece

Systematic production of biodiesel fuel from palm oil over porous K_2O@CaO catalyst derived from waste chicken eggshell via RSM/kinetic/thermodynamic studies

Panya Maneechakr *, Surachai Karnjanakom *

Department of Chemistry, Faculty of Science, Rangsit University, Pathumthani 12000, Thailand

ARTICLE INFO

Keywords:
Fatty acid methyl ester
Palm oil
Waste eggshell
K_2O@CaO catalyst
Transesterification

ABSTRACT

Sustainable synthesis of biodiesel fuel or fatty acid methyl ester (FAME) was studied via transesterification of palm oil (PO) over green/low-cost heterogeneous alkali (waste chicken eggshell/WCE) catalyst. The porous K_2O@CaO catalyst was effectively prepared via one-pot hydration-dehydration-incorporation process. The following reformations of catalyst properties were characterized by BET, XRD, SEM-EDX, TGA, FT-IR and CO_2-TPD techniques. As obtained results, the as-modified catalysts with characteristic properties such as stronger basic site, higher basicity and surface area were successfully achieved when compared with pristine/commercial CaO, resulting in more facile upgrading of PO to FAME product. An integration between 2^k factorial process with Box-Behnken model found that significant factors was in the order of catalyst loading amount > reaction time > reaction temperature. Meanwhile, the obtained optimal conditions were catalyst loading amount = 3 wt% of oil, molar ratio of methanol to oil = 15:1, reaction temperature = 80 °C and reaction temperature = 2 h, imparting a maximum FAME yield of 87.5%. For kinetic and thermodynamic studies of 10%KI/CaO catalyzed transesterification of PO, the important parameters such as Ea, A, ΔH, ΔS and ΔG were found to be 40.04 kJ/mol, 2.85×10^2 min^{-1}, 37.24 kJ/mol, − 172.61 J/mol.K and 60.97 kJ/mol, respectively. The calcium glyceroxide was easily formed during reusability test, resulting in a significant reduction of FAME yield. Thus, regeneration-calcination process at 800 °C was applied to fully recover its properties and catalytic performance. This work provided the eco-friendly strategy for FAME production which could be possibly applied in practical process.

1. Introduction

Owing to swift expansion of population, technology and industry, worldwide consumption of energy-fossil fuels is expanding year by year [1]. Thus, it is currently essential to rummage with alternative sources such as hydrogen, solar or wind energy and biodiesel fuel [2]. Among them, biodiesel fuel or fatty acid methyl ester (FAME) can be utilized to substitute the petroleum diesel since their some properties are quite analogous [3]. FAME is also revealed as an eco-friendly fuel including easily biodegradable, low toxic-smoke emission, high oxidative stability and natural lubricity [4]. As known that FAME can be synthesized by transesterification of vegetable oil or triglyceride molecule with alcohols over acid-base catalysts [5]. In commercial, homogeneous alkali catalysts such as NaOH and KOH are traditionally applied for upgrading of vegetable oil to FAME via transesterification process [6]. Even though these catalysts provide fast reaction rate with high yield of FAME but they cannot be reused, and the process requires high production cost for purification-washing technique. Moreover, they also present high sensitivity for saponification between free fatty acid and water in triglyceride oil, leading to facile formation of soap with significant decrease in FAME yield [7]. Heterogeneous catalysts propose a radical good chance to make the FAME production process more reasonable in an excellent direction. Their several advantages including non-corrosive, environmentally benign and reusable have been found, for instance, spent catalyst can be comfortably separated and recovered from reaction system via filtration or centrifugation without purification process [8–10]. More interestingly, their physicochemical properties can be easily modified to improve the catalytic performance and stability.

Recently, a range of heterogeneous alkali catalysts such as KOH/activated carbon, KOH/ZSM-5, KOH/MgO, CaO/SiO_2, ZrO_2-La_2O_3, K_2CO_3 and Na_2CO_3 have been developed and applied for FAME

* Corresponding authors.
E-mail addresses: panya.m@rsu.ac.th (P. Maneechakr), surachai.ka@rsu.ac.th (S. Karnjanakom).

https://doi.org/10.1016/j.jece.2021.106542
Received 26 June 2021; Received in revised form 5 October 2021; Accepted 7 October 2021
Available online 10 October 2021

production [11–16]. Among them, CaO is one of eco-friendly/low price/effective catalysts for FAME production owing to its high catalytic performance including high basicity- basic strength and low solubility in transesterification system [17]. CaO can be produced from natural source or waste materials such as waste egg shell, scallop shell, coralline shell, mussel shell and/or animal bones, which is not only reduce cost and conserve resource, but also retain the environmental problems [18]. Sirisomboonchai et al. [19] found that CaO (5 wt% of oil) derived from calcined scallop shell had proficient for producing the FAME with a high yield of 86% via transesterification at 65 °C for 2 h. Goli and Sahu [20] reported that high basicity and large number of basic sites at the edges of CaO cluster is one of key parameters to enhance the catalytic activity for transesterification of soybean oil. However, main problems for application of pristine CaO are still appeared, for instance, it has low surface area, resulting in lower number of disclosed active sites. Also, the natural deactivation can easily occur from interaction between of CaO with free fatty acids or water, leading to the leaching of calcium species together with soap formation. Thus, it is necessary to improve the CaO performances including surface area, stability and basicity [21]. Recently, one-pot hydration-dehydration process have been identified as an environmentally friendly method for pretreatment of CaO structure. Asikin-Mijan et al. [22] reported that hydrated-dehydrated CaO clamshell exhibited a high potential in the biodiesel production based on the increased of surface area and the basicity. Roschat et al. [23] found that the stronger basic site of new CaO are generated with the increase to some extent after hydration-dehydration process, resulting higher catalytic activity in transesterification process. Some metal doping on CaO can be also considered as an excellent way for improving the catalyst activity and stability. Zhang et al. [24] modified CaO catalyst by doping with CeO_2, and the catalytic results found that CeO_2 could stabilize the active phases, improving the stability of the catalyst during the reactions. Previously, Jairam et al. [25] found that the oyster shell impregnated by KI had excellent performance for transesterification of soybean oil (~85% conversion) at low temperature at 60 °C for 4 h. Mahesh et al. [26] and Komintarachat et al. [27] reported that impregnation of KBr and KCl on CaO structure significantly enhanced the catalytic activity for transesterification. Based on these details, the existence of K species on CaO catalyst is very important for generating new basic sites. However, the main problem of modified CaO is the apparent presence of low surface area, resulting in hard encounter between triglyceride molecules and active sites. It is challenging for development of new active catalyst such porous CaO along with the presence of K species for application in biodiesel production process.

Based on above details, it is very interesting to combine both methods for catalyst preparation. In this work, porous K_2O@CaO derived from waste chicken eggshell (WCE) was modified via one-pot hydration-dehydration-incorporation process, and applied for catalytic transesterification of PO to FAME product. It should be noted that KI was used as a substrate for K_2O formation on CaO support/catalyst during catalyst preparation process. The textural, morphological and chemical properties of as-prepared catalyst were characterized and discussed by BET, XRD, SEM-EDX, TGA, FT-IR and CO_2-TPD techniques. The roles of calcination temperature, catalyst type, KI doping amount was studied and discussed in details. The optimization process via an integration between 2^k factorial with Box-Behnken model was investigated in the existence of significant factors such as catalyst loading amount, reaction time and reaction temperature. This process is identified as a regression technique for solving environmental problems involving the response factors, which are affected in complex routes [28]. The main advantages for RSM applied in this work are revealed as follows: (I) it is the potential technique for forecasting the input–output relationships of catalytic transesterification systems by considering factor interactions such as reaction time, reaction temperature or catalyst loading amount, and (II) the production cost of FAME can be significantly reduced since lower experimental number were fixed under quadratic models [29]. Kinetic and thermodynamic studies for transesterification of PO catalyzed by K_2O@CaO were carried out to access the catalytic behaviors via pseudo-first order, Arrhenius and Eyring plots. The reusability test was also performed for 5 cycles under optimal conditions. This research provided an eco-friendly strategy with a low-cost for selective production of FAME fuel, which highly expected to further develop and apply in industrial-scale.

Table 1
Experimental conditions and FAME product yields studied via 2^4 factorial process for sustainable production of FAME from transesterification of PO over 10% KI/CaO catalyst.

Run	X_1 (°C)	X_2 (min)	X_3 (wt% of PO)	X_4 (mol/mol)	FAME yield (%)
1	60 (−1)	30 (−1)	1.0 (−1)	15:1 (−1)	29.5
2	90 (1)	30 (−1)	1.0 (−1)	15:1 (−1)	48.3
3	60 (−1)	180 (1)	1.0 (−1)	15:1 (−1)	52.7
4	90 (1)	180 (1)	1.0 (−1)	15:1 (−1)	58.5
5	60 (−1)	30 (−1)	4.0 (1)	15:1 (−1)	68.3
6	90 (1)	30 (−1)	4.0 (1)	15:1 (−1)	83.2
7	60 (−1)	180 (1)	4.0 (1)	15:1 (−1)	86.4
8	90 (1)	180 (1)	4.0 (1)	15:1 (−1)	84.1
9	60 (−1)	30 (−1)	1.0 (−1)	30:1 (1)	28.8
10	90 (1)	30 (−1)	1.0 (−1)	30:1 (1)	47.7
11	60 (−1)	180 (1)	1.0 (−1)	30:1 (1)	55.1
12	90 (1)	180 (1)	1.0 (−1)	30:1 (1)	59.2
13	60 (−1)	30 (−1)	4.0 (1)	30:1 (1)	68.2
14	90 (1)	30 (−1)	4.0 (1)	30:1 (1)	79.1
15	60 (−1)	180 (1)	4.0 (1)	30:1 (1)	83.5
16	90 (1)	180 (1)	4.0 (1)	30:1 (1)	82.8

The parameters are coded as follows: X1 = reaction temperature (°C), X2 = reaction time (min), X3 = catalyst loading amount (wt% of PO) and X4 = molar ratio of MeOH to PO (mol/mol).

2. Experimental

2.1. Material and chemicals

Refined palm oil (PO) from Morakot Industries Co., Ltd. Thailand was utilized as an oil feedstock for FAME production. Waste chicken eggshell (WCE) was collected from local restaurant in Bangkok and Pathumthani, Thailand, and used as a substrate for catalyst preparation. The commercial CaO was purchased from Ajax Finechem Pty Ltd. The chemical reagents such as KI (≥ 99.0%) and methyl heptadecanoate (≥ 99.0%) were purchased from Sigma-Aldrich company.

2.2. Catalyst preparation

WCE is washed with distilled water, crushed and sieved with a size around of 0.5–0.8 mm. The chemical compositions in WCE were determined using an energy dispersive X-ray spectrometer (XRF-Phillips, PW 2400), and the results are shown in Table S1. To produce CaO_{pris}, WCE was calcined at 800 °C for 2 h with a heating rate of 10 °C/min under air atmosphere. For comparison, the commercial CaO purchased from Ajax Finechem Pty Ltd was denoted as CaO_{com}. For doping-modification process, CaO_{pris} was further pretreated out via one-pot hydration-dehydration-incorporation technique [30]. Firstly, a certain amount of KI (2.5, 5.0, 10.0 or 20.0 wt%) was dissolved with distilled water. The CaO_{pris} was added in the as-prepared solution, then refluxed at 60 °C for 6 h. During this step, the CaO was simultaneously hydrated and deposited into KI/$Ca(OH)_2$ sample. Thereafter, the obtained sample was dried at 120 °C for overnight. Finally, it was calcined at 800 °C for 2 h with a heating rate of 10 °C/min under air atmosphere. Here, KI/Ca

Table 2
Experimental conditions and FAME product yields studied via Box-Behnken model for sustainable production of FAME from transesterification of PO over 10%KI/CaO catalyst.

Run	X_1 (°C)	X_2 (min)	X_3 (wt% of PO)	FAME yield (%)	
				Observed	Predicted
1	60 (−1)	30 (−1)	2.5 (0)	48.4	44.9
2	90 (1)	30 (−1)	2.5 (0)	63.6	65.1
3	60 (−1)	180 (1)	2.5 (0)	59.7	58.2
4	90 (1)	180 (1)	2.5 (0)	64.8	68.3
5	60 (−1)	105 (0)	1.0 (−1)	47.9	53.5
6	90 (1)	105 (0)	1.0 (−1)	64.1	64.6
7	60 (−1)	105 (0)	4.0 (1)	56.5	56.0
8	90 (1)	105 (0)	4.0 (1)	80.8	75.2
9	75 (0)	30 (−1)	1.0 (−1)	65.5	63.5
10	75 (0)	30 (−1)	1.0 (−1)	79.4	75.4
11	75 (0)	180 (1)	4.0 (1)	69.7	73.7
12	75 (0)	180 (1)	4.0 (1)	76.2	78.3
13	75 (0)	105 (0)	2.5 (0)	85.5	85.8
14	75 (0)	105 (0)	2.5 (0)	86.1	85.8
15	75 (0)	105 (0)	2.5 (0)	85.7	85.8

The parameters are coded as follows: X1 = reaction temperature (°C), X2 = reaction time (min) and X3 = catalyst loading amount (wt% of PO).

$(OH)_2$ was dehydrated, incorporated and decomposed into K_2O@CaO (denoted as 2.5–10.0%KI/CaO). It should be noted that CaO_{pris} pre-treated without KI doping was denoted as CaO_{pre}.

2.3. Catalyst characterization

The details in characterization method of as-prepared catalyst including BET, XRD, SEM-EDX, TGA, FT-IR and CO_2-TPD techniques are given in the Supporting Information (SI).

2.4. Catalytic transesterification of PO and analysis of FAME product

In this study, PO was used as a feedstock for FAME production. The catalytic transesterification was carried out under close system in order to avoid the leakage of MeOH gas during reaction. In a typical run, the certain amounts of catalyst and MeOH were added in a 50 mL glass tube reactor equipped with a thermocouple thermometer, and stirred at ambient temperature for 30 min. Thereafter, PO was added into the as-prepared system and transesterification reaction was performed. Here, critical roles of calcination temperature of WCE (500–900 °C), catalyst type, KI doping amount (2.5–20.0 wt%) were studied via transesterification of PO. The effect of reaction temperature (60–90 °C), reaction time (30–180 min), catalyst loading amount (1–4 wt% of PO) and molar ratio of MeOH to PO (15:1–30:1 mol/mol) were systematically investigated via an integration between 2^k factorial with Box-Behnken model (Tables 1 and 2). The details of experimental designs for FAME production are given in SI.

After the finishing reaction, the spent catalyst was separated from liquid product by centrifugation at 4000 rpm for 5 min. Prior reusability test, the collected spent catalyst was washed with acetone in order to eliminate some impurities. In the case of catalyst deactivation, it might be further regenerated by calcination at 800 °C for 2 h. The obtained FAME liquid at upper layer was purified by washing with distilled water unit its natural pH was obtained. Finally, the existence of water in FAME was evaporated at 110 °C. To analyze the yield of FAME product, gas chromatograph-flame ionization detector (GC-FID, Shimadzu GC-17A) equipped with a capillary column of DB-Wax (30 m × 0.25 mm × 0.25 μm) was applied using injector and detector temperatures of 250 ℃ and column temperature of 220 ℃. Here, EN 14103 standard method was used to quantify FAME yield using methyl heptadecanoate (C17:0) as an internal standard. All studies were carefully repeated for 3 times under the similar conditions. The FAME yield (%) was calculated as follows in Eq. (1):

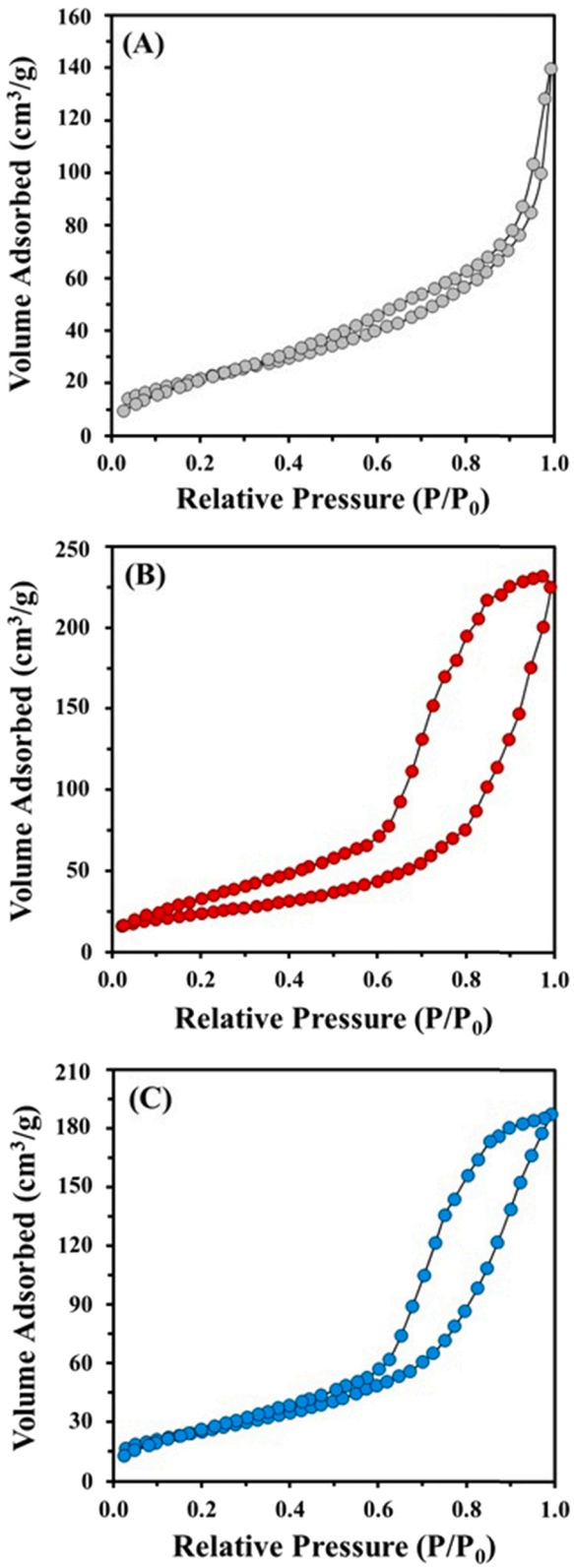

Fig. 1. N_2 sorption isotherms of (A) CaO_{pris}, (B) CaO_{pre} and (C) 10%KI/CaO.

Table 3
Physicochemical properties of various as-prepared catalysts.

Catalyst	Surface area (m^2/g)	Pore volume (cm^3/g)	Pore size (nm)	Crystallite size (nm)	Weak basic site (mmol/g)	Strong basic site (mmol/g)	Total basicity (mmol/g)
CaO_{pris}	10.2	0.17	9.8	54.2	0.521	0.056	0.577
CaO_{pre}	57.4	0.28	12.7	43.8	1.029	0.765	1.794
2.5%KI/CaO	55.1	0.25	12.6	40.6	1.124	0.843	1.967
5%KI/CaO	51.5	0.23	12.4	37.8	1.265	1.093	2.358
10%KI/CaO	46.3	0.19	12.1	34.4	1.407	1.359	2.766
20%KI/CaO	32.7	0.10	8.6	28.3	1.589	1.669	3.258
Spent 10%KI/CaO[a]	7.4	0.05	2.4	16.1	0.250	0.244	0.494
Spent 10%KI/CaO[b]	44.9	0.20	12.2	34.9	1.408	1.347	2.755
CaO_{com}	3.5	0.03	11.5	97.1	0.445	0.008	0.453

[a] Spent catalyst after recycling test for 5 cycles without regeneration.
[b] Spent catalyst after recycling test for 5 cycles with regeneration at calcination temperature of 800 °C for 2 h.

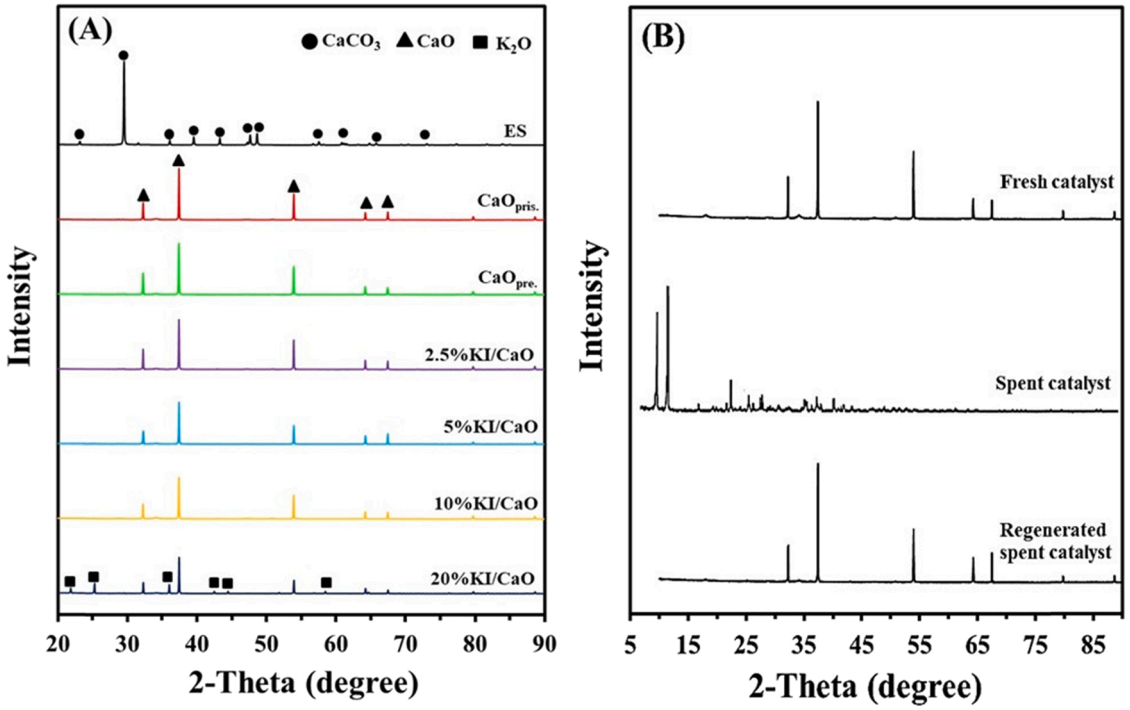

Fig. 2. XRD patterns of various catalysts.

$$\text{FAME yield}\ (\%) = \frac{(\sum A) - A_{EI}}{A_{EI}} \times \frac{C_{EI} \times V_{EI}}{W_S} \times \frac{W_{FAME}}{W_{PO}} \times 100 \quad (1)$$

where Σ*A* is the total peak areas of FAME, A_{EI} is the peak area of C17:0, C_{EI} is the concentration of C17:0 (mg/mL), V_{EI} is the volume of C17:0 (mL) and W_S is the weight of sample solution for GC (mg). W_P is the weight of FAME (mg) and W_O is the weight of PO.

3. Results and discussion

3.1. Characterization of catalyst and catalytic testing of transesterification

N_2 sorption isotherms of CaO_{pris}, CaO_{pre} and 10%KI/CaO are shown in Fig. 1. As obtained, the isotherms of all catalysts exhibited the irreversible type IV sorption isotherm, corresponding to mesoporous material [31]. For CaO_{pris}, the isotherm had a hysteresis loop shape, which was identified as type H3 with slit-shaped pores. After pretreatment and doping for CaO_{pre} and 10%KI/CaO, the isotherm with hysteresis loop shape was changed from H3 to H2, resulting from occurrence of ink-bottle mesoporous structure [32]. Meanwhile, their volumes and hysteresis loop space for N_2 adsorption was increased to some extent. It should be noted that narrower hysteresis loop of 10%KI/CaO was found when compared with CaO_{pre}, suggesting to K_2O dispersion inside/outside CaO structure. This phenomenon should be resulted from increasing of surface area, pore volume and pore size via hydration, dehydration and/or calcination occurred during pretreatment process as follows in Eqs. (2)–(4):

$$\text{Egg shell } CaCO_3 + 800\ ^\circ C \rightarrow CaO_{pris} + CO_2 \quad (2)$$

$$CaO + H_2O + 60\ ^\circ C \rightarrow Ca(OH)_2 \quad (3)$$

$$Ca(OH)_2 + 800\ ^\circ C \rightarrow \text{new } CaO_{pre} + H_2O \quad (4)$$

As such above results, the textural properties of various catalysts were also supported, and the results are shown in Table 3. One can see that the CaO_{pris} without any modification had a low surface area (10.2 m^2/g) and a small pore size (9.8 nm). In contrast, the surface area

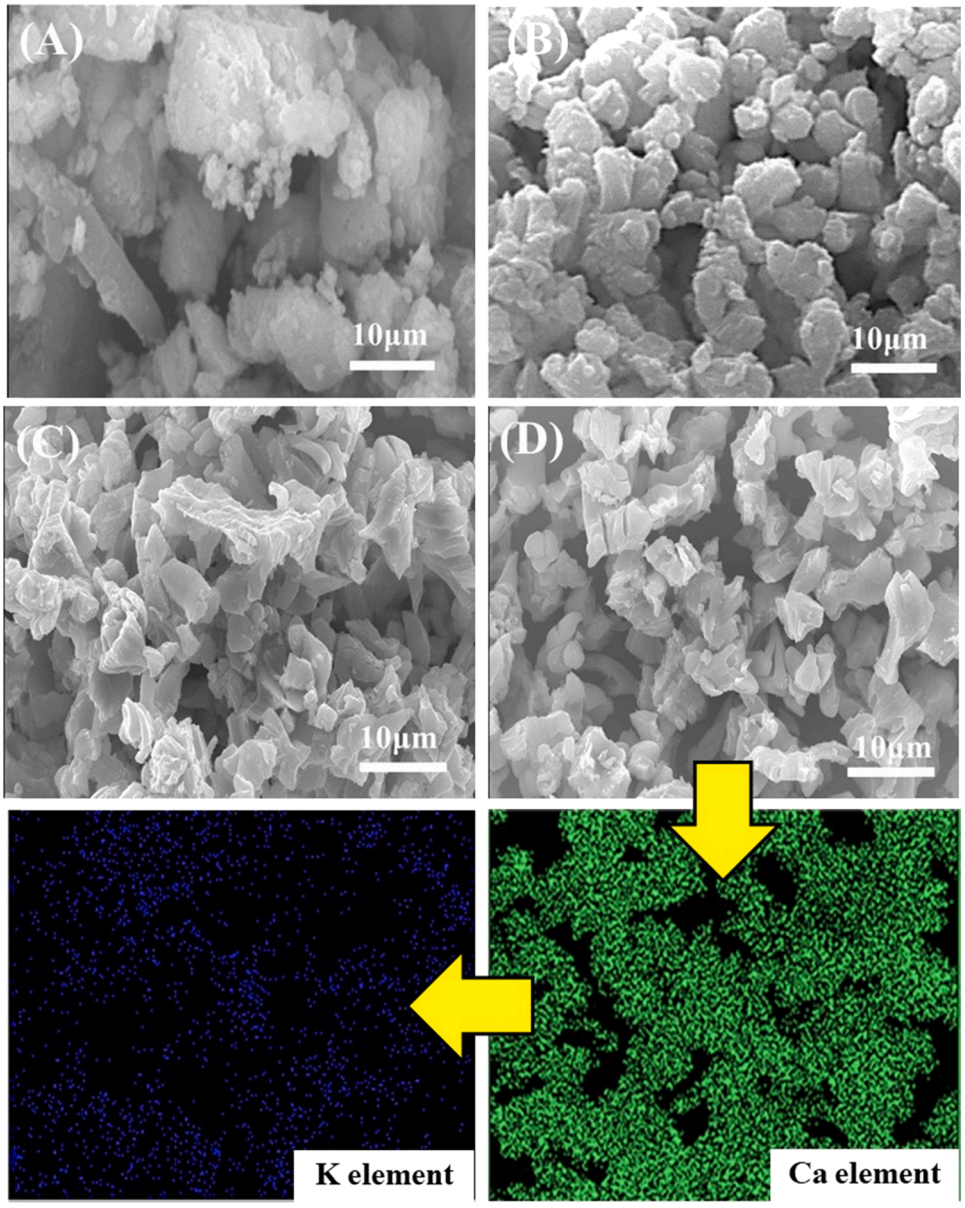

Fig. 3. SEM-EDS mapping images of (A) WCE, (B) CaO_{pris}, (C) CaO_{pre} and (D) 10%KI/CaO.

and pore size of CaO_{pre} were increased as expected up to 57.4 m^2/g and 12.7 nm, respectively. However, after KI doping, the surface areas of KI/CaO were continuously reduced from 55.1 to 38.7 m^2/g with the increasing of KI loading from 2.5 to 20 wt%. This suggests that CaO surface was partly occupied by the dispersed K_2O species. However, it should be noted that the reduction characteristic of surface number on catalyst/support was general pattern after metal loading was performed, resulting from some porous blockage. This phenomenon was in good agreement when compared with previous literatures [33,34]. That was why the effect of KI loading amount on CaO was also investigated. Herein, both K_2O and CaO could serve as synergistic active sites for PO transesterification reaction.

The XRD patterns of various catalysts are shown in Fig. 2A. One can see that the diffraction peaks of $CaCO_3$ was clearly appeared in WCE sample. Here, WCE could be completely converted into pure CaO after calcination at 800 °C. For all calcined samples, they presented the similar diffraction peaks at 32.45, 37.65, 53.88, 64.42 and 67.68°, corresponding to the CaO phase [35]. After pretreatment and KI doping from 2.5 to 20 wt%, the diffraction peaks of CaO with their crystallite size defined from Scherrer's equation were decreased to some extent (Table 3). This should be described on structural subtraction of CaO during pretreatment or covering by K_2O species at CaO structure. Interestingly, the strong diffraction peaks of K_2O phase were appeared in only 20%KI/CaO, suggesting that K_2O@CaO was easily accumulated owing to the sintering effect during the calcination when too much amount of K_2O was added [36]. In contrast, no bulks of K_2O were observed in the case of 2.5–10%KI/CaO, probably due to well dispersion of K_2O@CaO. The SEM image of various catalyst are shown in Fig. 3. The morphology of WCE exhibited irregular structure with larger particles, comparing with CaO_{pris}. After calcination, its surface became rougher while particle size was clearly decreased. Here, the highly textured CaO_{pre} was further found after hydration and dehydration at 800 °C. There was no significant difference when compared between CaO_{pre} with 10%KI/CaO. Also, excellent homogeneous dispersion of K species on the CaO structure was verified by EDX mapping image (Fig. 3). This was in good agreement with XRD results.

The DTG profile of WCE are shown in Fig. 4A. Initially, minor weight loss from 100° to 550°C was observed which should be due to

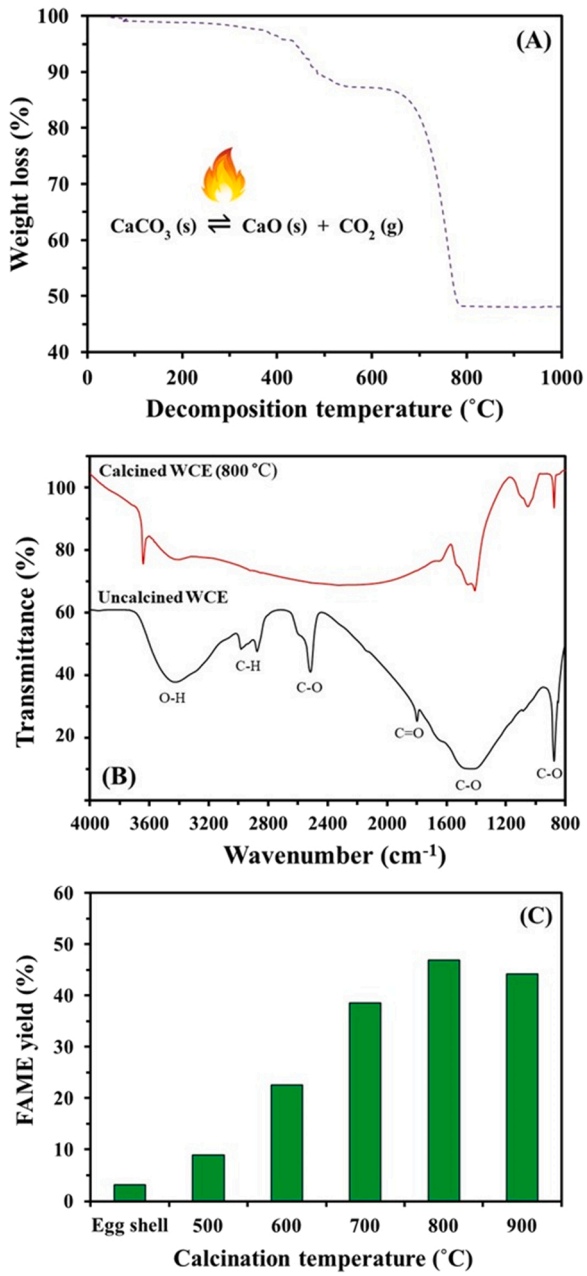

Fig. 4. (A) DTG profile of WCE, (B) FT-IR spectra of uncalcined WCE and calcined WCE and (C) Role of WCE calcined at different temperatures for sustainable production of FAME from transesterification of PO. Reaction conditions: catalyst loading amount = 1 wt% of oil, molar ratio of methanol to oil = 15:1, reaction temperature = 80 °C and reaction temperature = 2 h.

evaporation of water molecules and loss of protein/organic matter on WCE [37]. For major decomposition of $CaCO_3$ in WCE structure, it was found at temperature range of 600–800 °C with a total weight loss of 40.5% which was attributed to thermal decomposition of $CaCO_3$ to CaO and CO_2 together with loss of inorganic impurities. It should be noted that no significant change at > 800 °C was observed, indicating that the calcination temperature at 800 °C was appropriate for CaO preparation from WCE. The FT-IR spectra of uncalcined WCE and calcined WCE are shown in Fig. 4B. For uncalcined WCE, one can see that the major absorption bands of $CaCO_3$ molecule appeared at 1750, 1446 and 875 cm^{-1} were assigned to C═O stretching, C—O stretching and C—O bending, respectively [38,39]. For peaks at 2513 and 3000–2800 cm^{-1}, they presented to the existences of bicarbonate and C—H functional groups in uncalcined WCE, respectively which occurred from protein/organic molecules in uncalcined WCE. In addition, the O—H functional groups derived from water molecule in uncalcined WCE and calcined WCE structures were appeared at 3800–3000 cm^{-1}. After calcination at 800 °C (calcined WCE), the pattern for FT-IR spectra of uncalcined WCE was totally changed, indicating that main composition of calcined WCE was CaO while protein/organic molecules were destroyed. Fig. 4C shows the role of WCE calcined at different temperatures for production of FAME from transesterification of PO. For WCE without calcination, only FAME yield of 3.2% was obtained, indicating that transesterification of PO could not achieve over $CaCO_3$ catalyst. The increasing of calcination temperatures from 500° to 800 °C resulted in more generation of FAME yield. This was probably due to increasing of catalyst basicity when $CaCO_3$ was transformed into CaO with the higher amount. However, the FAME yield was reduced from 46.9% to 44.2% when too high calcination temperature at 900 °C was applied for CaO preparation. This phenomenon should be described on sintering and agglomeration effects, leading to the caving-in of molecular skeleton in CaO structure [40]. Therefore, the WCE calcination at 800 °C was fixed as an optimal temperature for production of CaO catalyst.

The CO_2-TPD profiles of catalysts before and after reactions are presented in Fig. 5. Here, Two CO_2-desorption peaks at ~200 (low temperature) and ~300 (high temperature) °C were corresponded to weak basic sites and strong basic sites, respectively [41]. It is found that CaO_{pris} almost contained only one main desorption peak/weak basic site at low temperature. Interestingly, after pretreatment by hydration-dehydration process, new strong basic sites were regenerated, and the desorption peaks were also shifted to higher temperatures for CaO_{pre}. This indicates that new active sites or super basic active sites were successfully formed after CaO was hydrated and dehydrated. Meanwhile, during pretreatment process, large amount of water molecule from $Ca(OH)_2$ was incessantly removed, resulting in formation of higher surface area and larger porosity of catalyst, leading to the simultaneous increase of total basicity on catalyst as shown in Table 3. More interestingly, stronger basic sites and higher basicity were incessantly regenerated to some extent when KI amounts were substituted from 2.5 to 20 wt%. It should be noted that the stronger/higher basicity with the co-presence of Ca–O, K_2–O ion pairs and isolated oxygen anions were more beneficial for catalytic transesterification of PO. Fig. 6 shows the role of catalyst type for production of FAME from transesterification of PO. For comparison, CaO_{pre} exhibited better catalytic performance than CaO_{pris} and CaO_{com}, resulting from the obvious presence of higher basicity and surface area. This indicates that the pretreatment process of CaO was important before catalytic application. It should be noted that CaO_{pris} had still better activity for catalytic transesterification than CaO_{com}, probably due to the promoting via other metals naturally existed in WCE. After modification-doping process, the FAME yield was increased from 46.9% to 52.9% when 2.5%KI/CaO was utilized. When KI doping amount was increased to 10 wt%, the FAME yield was dramatically increased dramatically and reached to 68.2%. Anywise, excessive doping of 20%KI on CaO_{pre} resulted in the serious reduction of surface area, pore size and metal dispersion rate, leading to increasing of mass transfer resistance and decreasing in catalytic performance. Based on these results, the 10%KI/CaO catalyst was selected for further studies.

3.2. Role of 2^k factorial analysis in FAME production

The experimental conditions and FAME product yields studied via 2^K factorial process are presented in Table 1. As observed, FAMEs produced via transesterification of PO catalyzed by 10%KI/CaO were yielded in the range between 29.5% and 86.4%. Here, the highest and lowest yields were determined, according to levels of independent input factors. Fig. 7A shows the significant levels in each factor via normal probability plots versus estimated values. One can see that the three factors such as reaction temperature (X_1, °C), reaction time (X_2, min) and catalyst

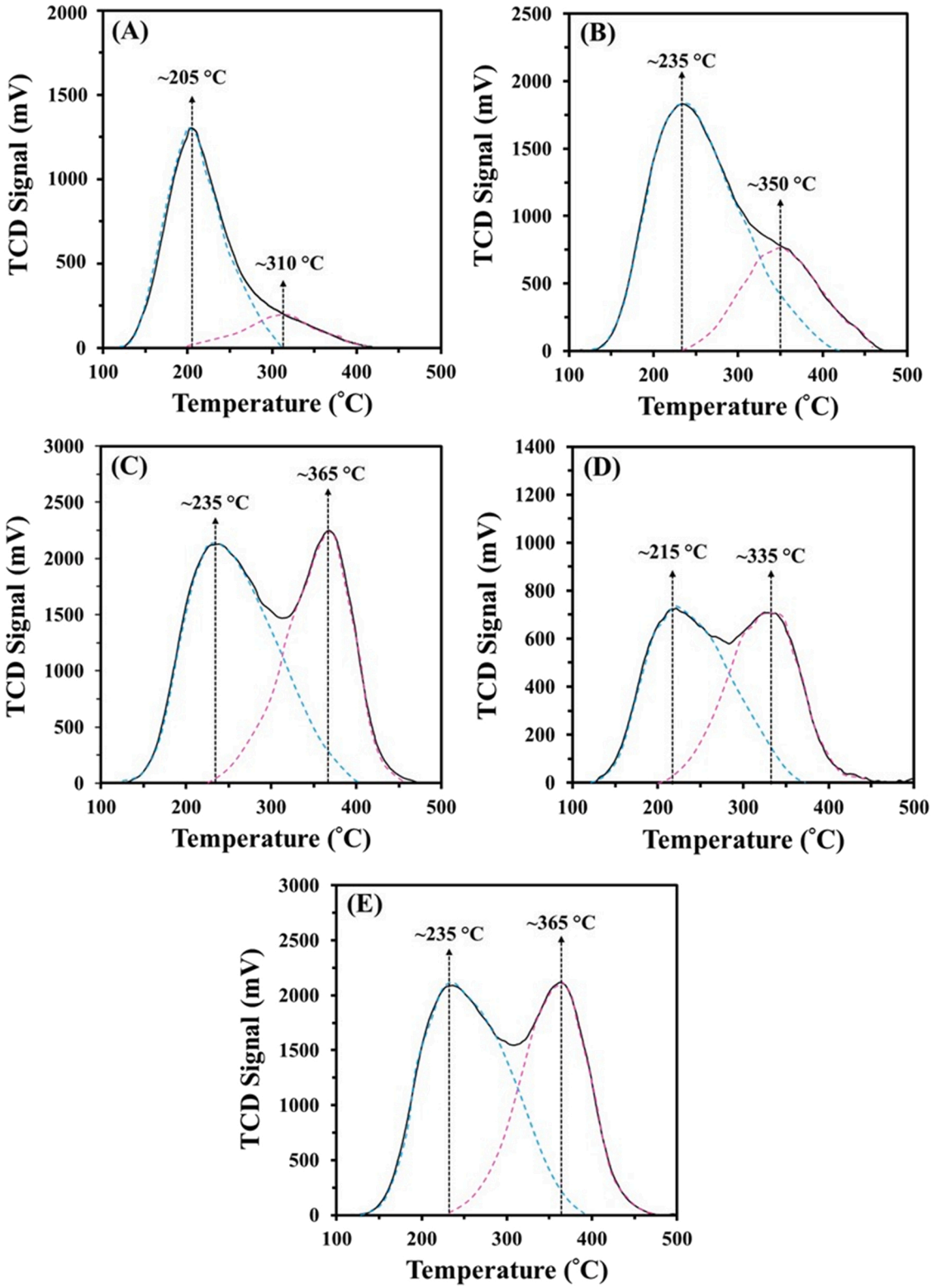

Fig. 5. CO_2-TPD profiles of (A) CaO_{pris}, (B) CaO_{pre}, (C) 10%KI/CaO, (D) spent 10%KI/CaO after reusability test for 5 times and (E) regenerated spent 10%KI/CaO.

loading amount (X_3, wt% of oil) including their interactions exhibited significant levels since they were obviously outward of the straight line. The factor abilities for FAME production rate were in the order of catalyst loading amount > reaction time > reaction temperature, indicating that the as-prepared 10%KI/CaO with loading amount was most important. Herein, the selected range of molar ratio of MeOH to PO (15:1–30:1 mol/mol) had non-significant effect for promoting the FAME yield occurred from transesterification of PO. According to Le Chatelier's principle, the application in MeOH with an excessive amount could improve the transesterification reaction towards the FAME formation [42]. Considering on economic portion, the remaining MeOH after complete reaction might be separated and recovered via evaporation-distillation-condensation process. Therefore, a minimum molar ratio of MeOH to PO (15:1) was adequate for this study. To

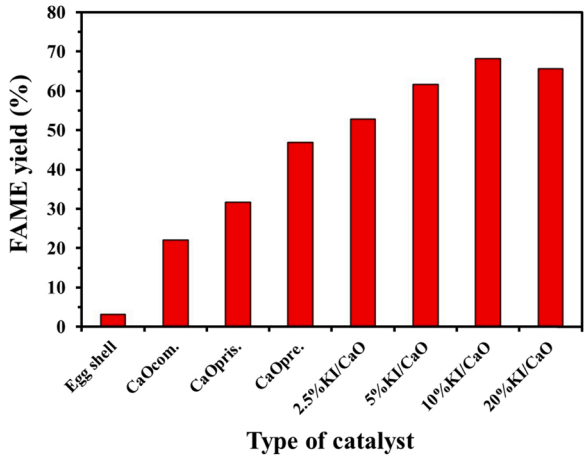

Fig. 6. Role of catalyst type for sustainable production of FAME from transesterification of PO. Reaction conditions: catalyst loading amount = 1 wt% of oil, molar ratio of methanol to oil = 15:1, reaction temperature = 80 °C and reaction temperature = 2 h.

support these data, the analysis of variance (ANOVA) was determined, and the results are shown in Table 4. The minimum, medium and maximum of sum of square values defined from reaction temperature, reaction time and catalyst loading amount were 309.76, 745.29 and 4089.60, respectively. The model terms were selected when $F_{critical}$ value was > 5.318. As expected, the normal probability plots were in good agreement with ANOVA results at 95% confident level with $F_{0.05}$. Thereafter, the linear regression model determined from 2^K factorial analysis was used to calculate the predicted FAME yield as follows in Eq. (5):

$$Y = 63{\cdot}46 + 4{\cdot}40X_1 + 6{\cdot}83X_2 + 15{\cdot}99X_3 - 3{\cdot}54X_1X_2 - 1{\cdot}55X_1X_3 - 2{\cdot}08X_2X_3 \quad (5)$$

Where *Y* is the FAME yield, X_1 is the reaction temperature (°C), X_2 is the reaction time (min), X_3 is the catalyst loading amount (wt% of PO).

Fig. 7B and C shows the normal probability plots of residual value versus pk × 100 and distribution plots of predicted FAME yield versus residual value. As predicted, the regression model presented a good linearity that a value of correlation coefficient was close to 1 (R^2 = 0.9445). Also, the distribution level of residue value was in the range of 0–4% while the distribution behavior was in a mess, indicating that the as-applied model had high precision.

3.3. Optimization of FAME production via Box-Behnken analysis

The experimental conditions and FAME product yields studied via from Box-Behnken design are presented in Table 2. The quadratic regression model including low, medium and high levels determined from Box-Behnken analysis with response surface methodology (RSM) was used to calculate the predicted FAME yield as follows in Eq. (6):

$$Y = 85.77 + 7.60X_1 + 4.11X_2 + 3.29X_3 - 18.51X_1^2 - 8.13X_2^2 - 4.93X_3^2 - 2.53X_1X_2 + 2.03X_1X_3 - 1.85X_2X_3 \quad (6)$$

Where *Y* is the FAME yield, X_1 is the reaction temperature (°C), X_2 is the reaction time (min), X_3 is the catalyst loading amount (wt% of PO).

The predicted FAME yields calculated from Eq. (6), and their results were close to observed FAME yields. Meanwhile, as shown in Fig. 8A and B, the value of $R^2 > 0.9$ was clearly found via the linear plots of observed FAME yield versus predicted FAME yield while distribution behavior was in disorder with level range of ± 7, suggesting that the regression model was had high precision with a variability of 94.32% for

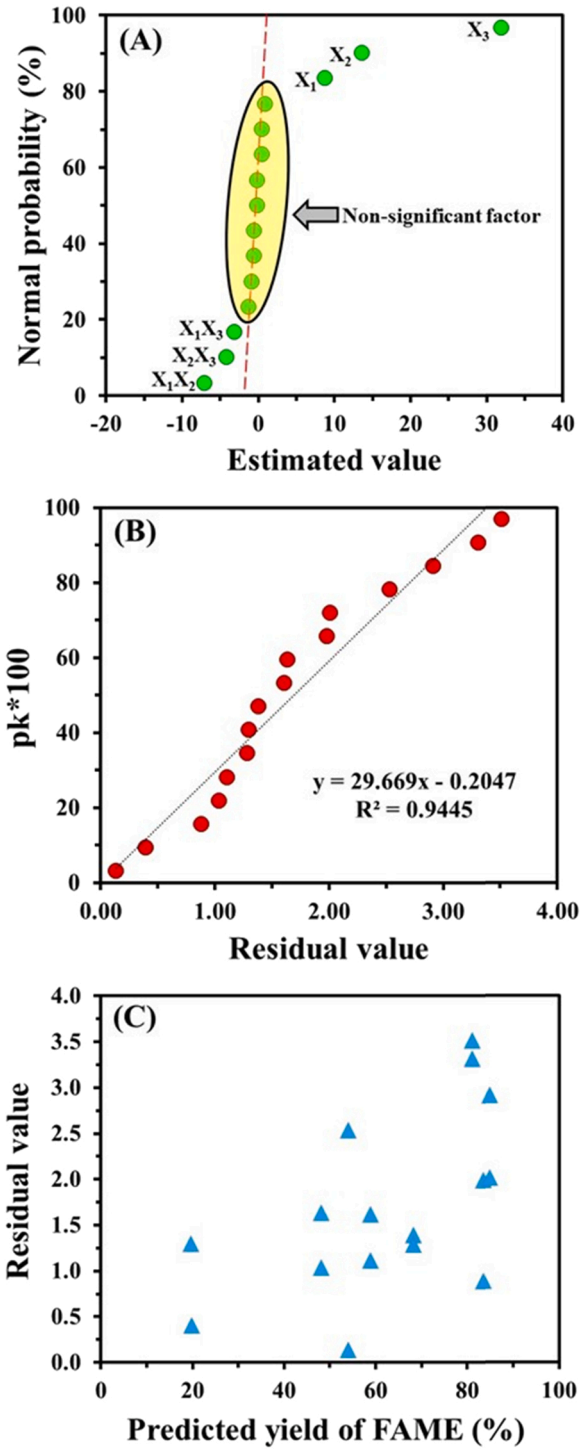

Fig. 7. (A) Normal probability, (B) linear regression and (C) distribution level plots derived from 2^4 factorial design for sustainable production of FAME from transesterification of PO over 10%KI/CaO catalyst.

polynomial study. To optimize the reaction conditions with a maximum FAME yield among the Box-Behnken analysis, the application using response surface 3D and contour plots for FAME production is shown in Fig. 9. Fig. 9A and D shows interaction between reaction temperature and reaction time for production of FAME from transesterification of PO catalyzed by 10%KI/CaO at a catalyst loading amount of 2.5 wt% of PO (medium level). The increasing of reaction temperature from 60° to 80 °C promoted the facile transesterification of PO for 120 min wherewith FAME yield increased from 60.7% to 86.9%. Here, natural viscosity

Table 4
Analysis of variance determined from 2^4 factorial process for sustainable production of FAME from transesterification of PO over 10%KI/CaO catalyst.

Source of variation	Sum of square	Degree of freedom	Mean square	F_{Value}	$F_{Critical}$
X_1	309.76	1	309.76	172.69	5.318
X_2	745.29	1	745.29	415.49	
X_3	4089.60	1	4089.60	2279.92	
X_4	2.72	1	2.72	1.52	
X_1X_2	200.22	1	200.22	111.62	
X_1X_3	38.44	1	38.44	21.43	
X_2X_3	68.89	1	68.89	38.41	
Error	14.35	8	1.79		
Total	5469.28	15			

The parameters are coded as follows: X1 = reaction temperature (°C), X2 = reaction time (min), X3 = catalyst loading amount (wt% of PO) and X4 = molar ratio of MeOH to PO (mol/mol).

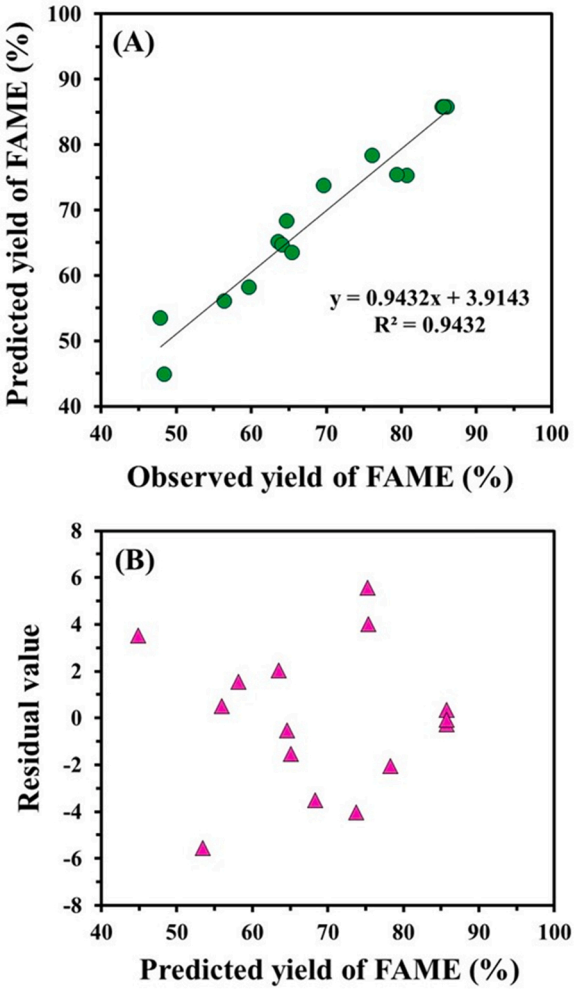

Fig. 8. (A) Quadratic regression and (B) distribution level plots derived from Box-Behnken design for sustainable production of FAME from transesterification of PO over 10%KI/CaO catalyst.

of PO should be decreased with the increasing in mass-transfer distribution and collision frequency between PO-MeOH-catalyst multiphase reaction system when higher reaction temperature was applied. However, a few reductions of FAME yield were observed at > 80 °C, probably due to MeOH conversion from liquid phase to gas phase wherewith difficult to be condensed again, resulting in no available for transesterification reaction [43]. In the case of reaction time, it exhibited the same pattern such the effect of reaction temperature. When the times were reached to 30–120 min, the FAME yield increased to around 75–87% thereafter slightly reduced to some extent. This is possible that the backward reaction may be replaced to forward reaction with too long reaction time since transesterification of PO was equilibrium reaction [44].

Fig. 9B and E shows interaction between reaction temperature and catalyst loading amount for production of FAME from transesterification of PO catalyzed by 10%KI/CaO at a reaction time of 105 min (medium level). Herein, a highest FAME yield of 87.2% could be obtained when reaction temperature of 80 °C and catalyst loading amount of 3.0 wt% of PO were achieved. It should be noted that the catalyst loading amount was never exceed than 3.0 wt% even the interaction between reaction time and catalyst loading amount was applied for FAME production (Fig. 9C and F). As known that too high loading amount of catalyst resulted in a poor mixing owing to the high viscosity of the mixture of reactants and catalyst, leading to the increasing in mass transfer resistance in reaction system [45]. Also, the saponification could be easily occurred with too high basicity (> 10%KI doping) or too much loading amount of catalyst (> 3 wt% of PO), leading to significant reduction of FAME yield. Based on RSM analysis, the optimization at equilibrium conditions was systematically determined using Box-Behnken design with quadratic regression model. As predicted, a maximum FAME yield of 87.9% was obtained under optimal conditions: catalyst loading amount = 3 wt% of oil, molar ratio of methanol to oil = 15:1, reaction temperature = 80 °C and reaction temperature = 2 h via an integration of Box-Behnken design with quadratic regression model. To guarantee the precision of this design, the actual experiments were carefully carried out for three replications under the optimal conditions. As expected, an average FAME yield of 87.5% from actual experiments was achieved which was acceptable for this study.

3.4. Kinetic and thermodynamic behaviors for FAME production

The possible reaction pathways for transesterification of PO into FAME over K_2O@CaO catalyst are shown in Fig. 10. Firstly, an anion of methoxide/nucleophile was formed via reaction between K_2O@CaO with MeOH. During reaction, carbonyl groups of PO was attacked by methoxide ions to form an intermediate of carbonyl alkoxy. Then, this intermediate was rearranged to produce the FAME product while alkoxide ion occurred on the glycerol backbone was immediately protonated to form hydroxyl group [46]. Lastly, the diglyceride and monoglyceride groups were further interacted with methoxide anions via the same pathways to produce 3 mols of FAMEs and 1 mol of glycerol. Based on these reactions, a kinetic behavior for K_2O@CaO catalyzed transesterification of PO was further studied under different reaction times (40–120 min) and reaction temperatures (50–80 °C) while the other factors such as catalyst loading amount (3 wt% of PO) and molar ratio of MeOH to PO (15:1 mol/mol) were kept constant. The transesterification stoichiometries including the three steps: triglyceride (TG), diglyceride (DG) and monoglyceride (MG) reacted with MeOH to form FAME product are provided in Eqs. (7–9). The overall of FAME and glycerol (GR) formations is given as follows in Eq. (10) [47]:

$$TG + MeOH \underset{k_4}{\overset{k_1}{\leftrightarrow}} FAME + DG \quad (7)$$

$$DG + MeOH \underset{k_5}{\overset{k_2}{\leftrightarrow}} FAME + MG \quad (8)$$

$$MG + MeOH \underset{k_6}{\overset{k_3}{\leftrightarrow}} FAME + GR \quad (9)$$

$$TG + 3MeOH \underset{k_8}{\overset{k_7}{\leftrightarrow}} 3FAME + GR \quad (10)$$

As mentioned above, the PO conversion to FAME was defined as the total moles of FAME divided by the TG moles, while transesterification

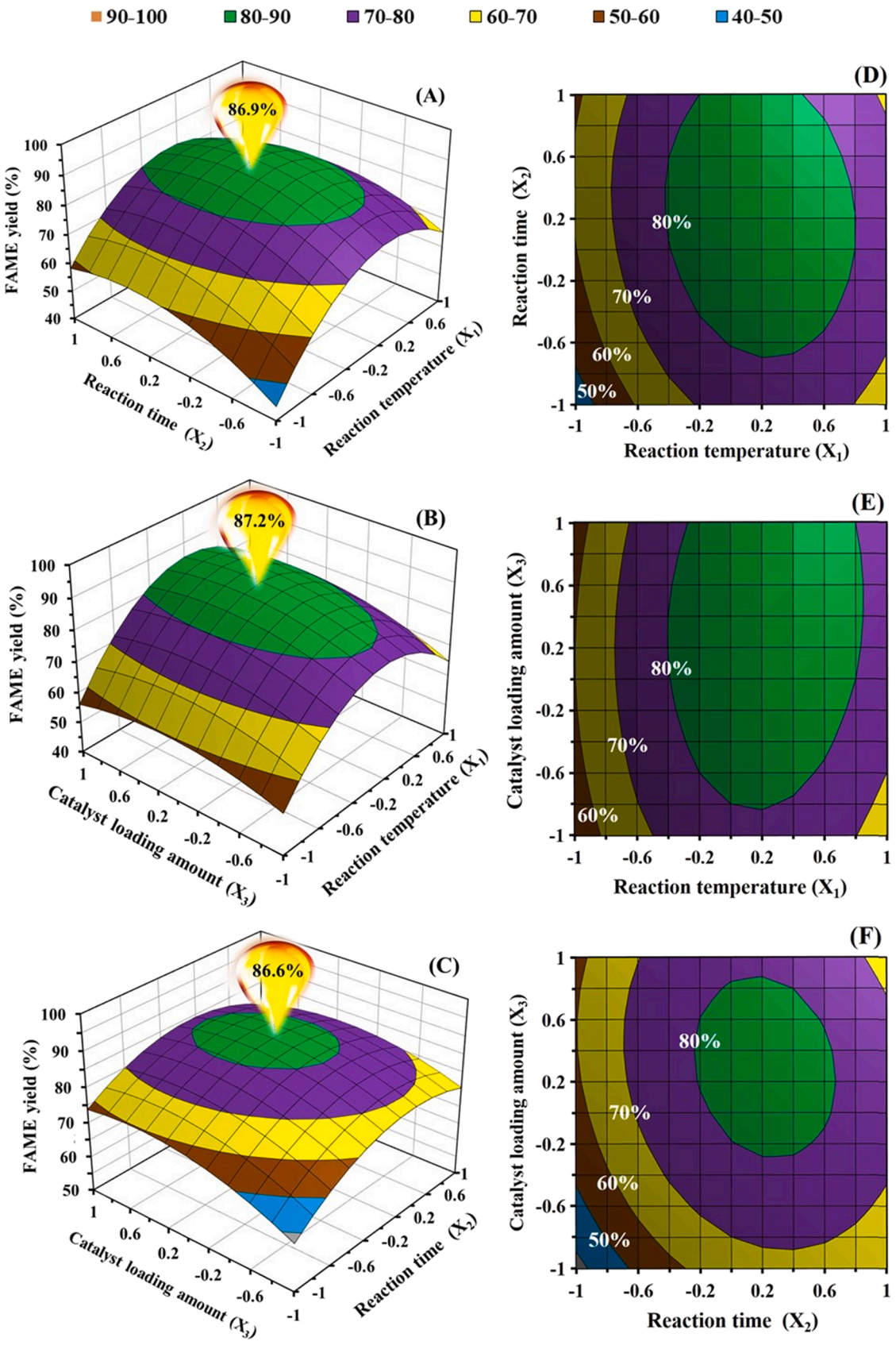

Fig. 9. Response surface 3D and contour plots derived from Box-Behnken design for sustainable production of FAME from transesterification of PO over 10%KI/CaO catalyst: (A,D) interaction plot between reaction temperature with reaction time, (B,E) interaction plot between reaction temperature with catalyst loading amount, and (C,F) interaction plot between reaction time with catalyst loading amount.

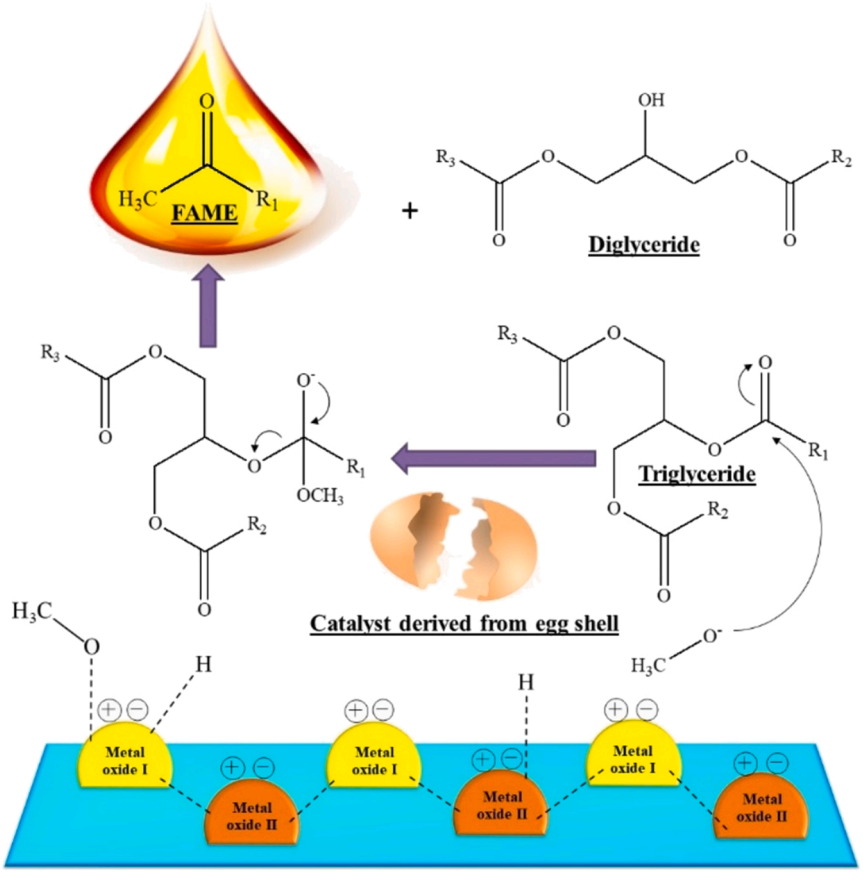

Fig. 10. Possible reaction mechanism of CaO-catalyzed transesterification of PO/triglyceride into FAME.

rate was as follows in Eq. (11):

$$-\frac{dC_A}{dt} = k_7 C_A^X C_B^Y - k_8 C_C^W C_D^Z \quad (11)$$

where C_A, C_B, C_C and C_D are the concentrations of TG, MeOH, GR and FAME, respectively, while W, X, Y and Z are to their reaction orders. k_7 and k_8 are the kinetic constants for the forward and backward reactions, respectively.

Owing to reversible process of transesterification mechanism, excessive concentration of MeOH was utilized to push the forward equilibrium. In the other words, the utilized amount of MeOH was much higher than another one. Here, $k_7 C_B{}^Y$ could be invariable where $k' = k_7 C_B{}^Y$ or k' is the altered rate constant. Furthermore, k_8 should be excised since their components were much lower than k_7. Therefore, from Eq. (11), it could be rewritten as follows in Eq. (12):

$$-\frac{dC_A}{dt} = k' C_A^X \quad (12)$$

From Eq. (12), it could be further integrated and rearranged over the PO conversion in the case that $n = 1$ as follows in Eq. (13):

$$-\ln(1-X_{PO}) = k't \quad (13)$$

where X_{PO}, k' and t are the PO conversion, reaction rate constant and reaction time, respectively. The k' value was calculated from the slope by plotting $-\ln(1-X_{PO})$ versus t at various reaction temperatures (T).

In the case that n ‡ 1, it should be modified by $k' = k'/C_{A0}$, which should be expressed as follows in Eq. (14):

$$(1-X_{PO})^{(1-n)} = 1+(n-1)k'C_{A0}{}^n t \quad (14)$$

To examine the activation energy (Ea) occurred during catalytic upgrading of PO over 10%KI/CaO, the Arrhenius model was purposed and given as follows in Eq. (15):

$$k' = A\exp\frac{-Ea}{RT} \quad (15)$$

where A is the pre-exponential factor (min^{-1}), R is the universal gas constant (8.314 J/K.mol) According to Eq. (15), Ea value was determined by plotting ln k' versus 1/T. Thus, it should be rewritten to linear form as follows in Eq. (16):

$$lnk' = -\frac{E_a}{RT} + lnA \quad (16)$$

The thermodynamic behaviors including enthalpy change (ΔH), entropy change (ΔS) and Gibbs free energy (ΔG) for 10%KI/CaO catalyzed transesterification of PO were investigated using Eyring-Polanyi model as follows in Eq. (17) [43]:

$$k' = \frac{k_b T}{h}\exp\frac{-\Delta G}{RT} \quad (17)$$

From Eq. (17), the values of ΔH and ΔS was determined by plotting ln (k'/T) versus 1/T. Thus, it should be rewritten to linear form as follows in Eq. (18):

$$\ln\left(\frac{k'}{T}\right) = -\frac{\Delta H}{RT} + \ln\left(\frac{k_b}{h}\right) + \frac{\Delta S}{R} \quad (18)$$

where k_b is the Boltzmann constant (1.3806×10^{-23}) and h is Planks constant (6.626176×10^{-34}).

The values of ΔG in each temperature were calculated as follows in Eq. (19):

$$\Delta G = \Delta H - T\Delta S \quad (19)$$

Fig. 11 A shows the correlation between $-\ln(1-X_{PO})$ and reaction time

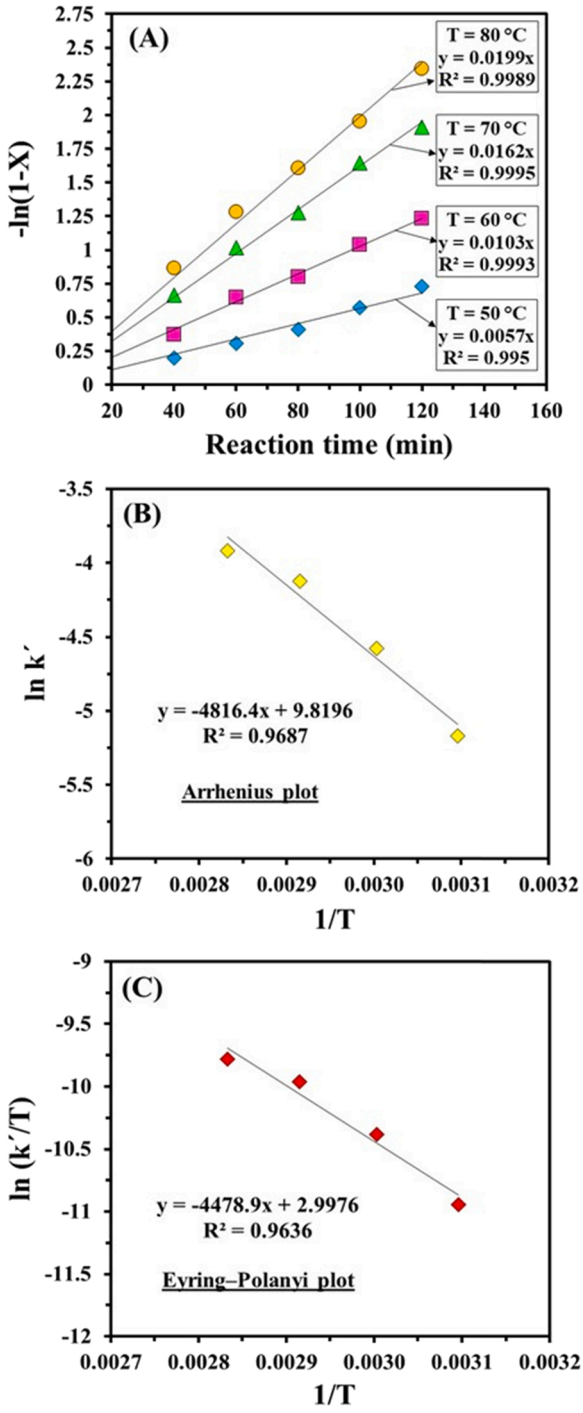

Fig. 11. (A) Kinetic logarithms of at various temperatures (50–80 °C) and times (40–120 min), (B) Arrhenius plot of ln k´ vs. 1/T and (C) Eyring-Polanyi plot of ln(k´/T) vs. 1/T for sustainable production of FAME from transesterification of PO over 10%KI/CaO catalyst.

for transesterification catalyzed by 10%KI/CaO at different temperatures. One can see that a linear kinetic relationship was well accorded with the hypothesis of pseudo-first order ($R^2 > 0.99$) for FAME production. As shown in Table S2, the reaction rate constants were increased from 0.0057 to 0.0199 min^{-1} with the increasing of the reaction temperatures from 50° to 80°C, suggesting that the transesterification was generally required at higher temperature. Fig. 11B shows the Arrhenius plots of 1/T versus reaction rate constants. The activation energy and pre-exponential factor were found to be 40.04 kJ/mol, 2.85×10^2 min^{-1}, respectively. The performance of 10%KI/CaO

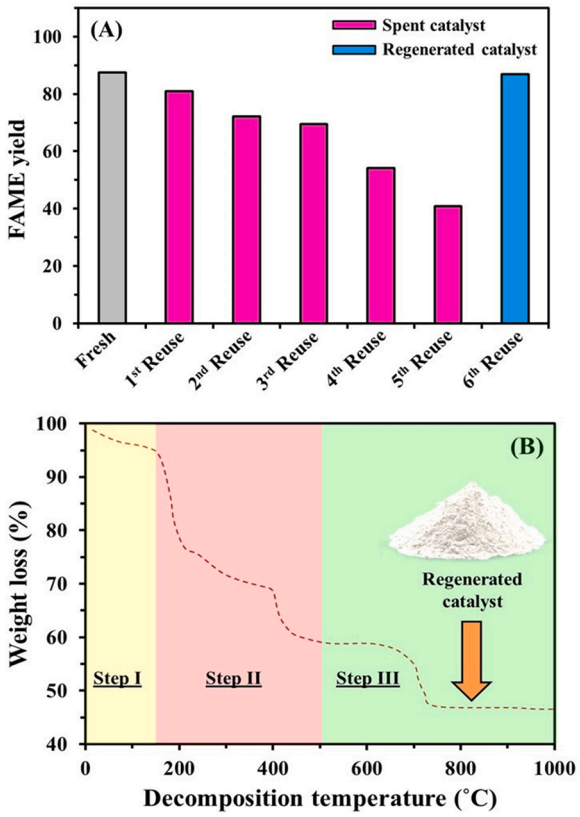

Fig. 12. (A) Reusability test of 10%KI/CaO catalyst for sustainable production of FAME from transesterification of CPO. Reaction conditions: catalyst loading amount = 3 wt% of oil, molar ratio of methanol to oil = 15:1, reaction temperature = 80 °C and reaction temperature = 2 h. (B) DTG profile of spent 10% KI/CaO after reusability test for 5 times.

catalyst in this study was also compared with previous literatures (Table S3) [48–53]. An activation energy of 10%KI/CaO catalyst promoted faster reaction rate which was in good agreement with the range 33–84 kJ/mol for transesterification of vegetable oils catalyzed by heterogeneous CaO catalysts [44]. Fig. 11C shows Eyring-Polanyi plot to determine thermodynamic parameters. Here, the values of ΔG, ΔH and ΔS were calculated, and the results are shown in Table S2. The ΔG in each temperature had positive values, indicating that the transesterification catalyzed by 10%KI/CaO were endergonic and unspontaneous reaction. Also, the endothermic nature was confirmed since ΔH had positive value of 37.24 kJ/mol [54]. Here, ΔS did not consider since MeOH was used in excessive amount. From these results, it summarizes that 10%KI/CaO catalyst exhibited high reactivity/pre-exponential factor, fast reaction rate and low activation energy/mass transfer resistance for transesterification of PO.

3.5. *Catalyst reusability*

The reusability of 10%KI/CaO catalyst was evaluated under the optimal conditions for six consecutive runs (Fig. 12A). From 1st to 5th cycles, the catalyst was recovered from the reaction mixture by centrifugation, and washed with acetone to eliminate some impurities without further regeneration process. It is found that FAME yield was still higher than 69%, indicating that the catalyst stability was remained during the three cycles. Unlikely, in 4th and 5th cycles, a serious decrease in catalytic performance was observed. This deactivation could be described in the change of CaO phase into calcium glyceroxide phase, resulting in the dramatic reduction of catalyst basicity [55]. Herein, the crystallite size of CaO was highly decreased from 34.4 to 2.0 nm with the increasing of cycle number from 1 to 5. The leaching amount of K_2O

species on catalyst was detected by EDX technique, and the results found that the difference percent of K_2O amount on catalyst between fresh one and spent one (5th cycle) was < 1.5 wt%, indicating that main problem of catalyst deactivation was mainly occurred from changing of CaO phase. These phenomena were also confirmed by XRD and CO_2-TPD results (Figs. 2B, 5D-E and Table 3). Therefore, it was necessary to be regenerated by calcination process. Fig. 12B shows the DTG profile of spent catalyst in form of calcium glyceroxide. Initially, minor weight loss at ~100 °C was assigned to general evaporation of moisture. Then, a strong exothermic effect with major decomposition of the glyceroxide anions to $CaCO_3$ was appeared at 150–450 °C [56]. Finally, CaO was obtained from $CaCO_3$ decomposition at 600–800 °C. Here, further increasing at > 800 °C had no significant change in DTG curve. Based on this study, regeneration of spent catalyst by calcination at 800 °C was applied. As expected after regeneration, the CaO phase with total basicity was restored, leading to significant enhancement of FAME yield in 6th cycle. In the other words, no serious reduction in the FAME yield was found when compared with the fresh one, suggesting that catalytic of the spent catalyst could be perfectly recovered using this regeneration method.

4. Conclusion

In summary, porous K_2O@CaO was successfully prepared and applied as a low-cost/effective catalyst for sustainable production of FAME from transesterification of PO. The surface area and pore size of CaO catalyst were well improved after hydration-dehydration, leading to regeneration of new basic site for catalytic upgrading of PO. The 10% KI/CaO presented better catalytic performance than CaO_{com}, CaO_{pris} and CaO_{pre} because it had higher basicity and/or stronger basic site, a maximum FAME yield of 87.9% was achieved under optimal conditions: catalyst loading amount = 3 wt% of oil, molar ratio of methanol to oil = 15:1, reaction temperature = 80 °C and reaction temperature = 2 h via an integration of 2^k factorial with Box-Behnken analyses. According to their kinetic and thermodynamic behavior, an activation energy for transesterification catalyzed by 10%KI/CaO was 40.04 kJ/mol which was endergonic/unspontaneous/endothermic reaction. The deactivation problem of spent catalyst could be solved by calcination at 800 °C. This is expected that such catalysts could be widely applied for sustainable production of FAME in practical process.

CRediT authorship contribution statement

Panya Maneechakr: Conceptualization, Formal analysis, Validation. **Surachai Karnjanakom:** Project administration, Methodology, Formal analysis, Writing – original draft, Writing – review & editing.

Declaration of Competing Interest

The authors declare that they have no known competing financial interests or personal relationships that could have appeared to influence the work reported in this paper.

Acknowledgments

The authors would like to gratefully appreciate Department of Chemistry, Faculty of Science, Rangsit University, Thailand for supporting all chemicals, equipment and instruments.

Appendix A. Supporting information

Supplementary data associated with this article can be found in the online version at doi:10.1016/j.jece.2021.106542.

References

[1] P. Maneechakr, S. Karnjanakom, Improving the bio-oil quality via effective pyrolysis/deoxygenation of palm kernel cake over a metal (Cu, Ni, or Fe)-doped carbon catalyst, ACS Omega 6 (2021) 20006–20014.
[2] A.S. Yusuff, A. Gbadamosi, L.T. Popoola, Biodiesel production from transesterified waste cooking oil by zinc-modified anthill catalyst: parametric optimization and biodiesel properties improvement, J. Environ. Chem. Eng. 9 (2021), 104955.
[3] B. Karmakar, G. Halder, Progress and future of biodiesel synthesis: advancements in oil extraction and conversion technologies, Energy Convers. Manag. 182 (2019) 307–339.
[4] N. Ishak, J. Estephane, E. Dahdah, L.M. Chalouhi, S. Nassreddine, B.E. Khoury, S. Aouad, Outstanding activity of a biodiesel coated K2O/fumed silica catalyst in the transesterification reaction, J. Environ. Chem. Eng. 9 (2021), 104665.
[5] M. Athar, S. Zaidi, A review of the feedstocks, catalysts, and intensification techniques for sustainable biodiesel production, J. Environ. Chem. Eng. 8 (2020), 104523.
[6] R.N.R. Abdullah, D. Sianipar, I.F. Ariyani, Nata, conversion of palm oil sludge to biodiesel using alum and KOH as catalysts, Sustain. Environ. Res. 27 (2017) 291–295.
[7] I. Chanakaewsomboon, C. Tongurai, S. Photaworn, S. Kungsanant, R. Nikhom, Investigation of saponification mechanisms in biodiesel production: microscopic visualization of the effects of FFA, water and the amount of alkaline catalyst, J. Environ. Chem. Eng. 8 (2020), 103538.
[8] E.G.S. Junior, V.H. Perez, I. Reyero, A. Serrano-Lotina, O.R. Justo, Biodiesel production from heterogeneous catalysts based K_2CO_3 supported on extruded γ-Al_2O_3, Fuel 241 (2019) 311–318.
[9] S. Karnjanakom, A. Bayu, P. Maneechakr, C. Samart, S. Kongparakul, G. Guan, Simultaneous assistance of molecular oxygen and mesoporous SO_3H–alumina for a selective conversion of biomass-derived furfural to γ-valerolactone without an external addition of H_2, Sustain. Energy Fuels 5 (2021) 4041–4052.
[10] R. Bhoi, D. Singh, S. Mahajani, Investigation of mass transfer limitations in simultaneous esterification and transesterification of triglycerides using a heterogeneous catalyst, React. Chem. Eng. 2 (2017) 740–753.
[11] T.E. Odetoye, J.O. Agu, E.O. Ajala, Biodiesel production from poultry wastes: waste chicken fat and eggshell, J. Environ. Chem. Eng. 9 (2021), 105654.
[12] T. Saba, J. Estephane, B.E. Khoury, M.E. Khoury, M. Khazma, H.E. Zakhem, S. Aouad, Biodiesel production from refined sunflower vegetable oil over KOH/ZSM5 catalysts, Renew. Energy 90 (2016) 301–306.
[13] P. Maneechakr, S. Karnjanakom, A combination of 2^k factorial with Box-Behnken designs for FAME production via methanolysis of waste cooking palm oil over low-cost Catalyst, J. Environ. Chem. Eng. 7 (2019), 103389.
[14] K. Malins, The potential of K_3PO_4, K_2CO_3, Na_3PO_4 and Na_2CO_3 as reusable alkaline catalysts for practical application in biodiesel production, Fuel Process. Technol. 179 (2018) 302–312.
[15] H. Sun, Y. Ding, J. Duan, Q. Zhang, Z. Wang, H. Lou, X. Zheng, Transesterification of sunflower oil to biodiesel on ZrO_2 supported La_2O_3 catalyst, Bioresour. Technol. 101 (2010) 953–958.
[16] C. Samart, C. Chaiya, P. Reubroycharoen, Biodiesel production by methanolysis of soybean oil using calcium supported on mesoporous silica catalyst, Energy Convers. Manag. 51 (2010) 1428–1431.
[17] N.A. Zul, S. Ganesan, T.S. Hamidon, W.D. Oh, M.H. Hussin, A review on the utilization of calcium oxide as a base catalyst in biodiesel production, J. Environ. Chem. Eng. 9 (2021), 105741.
[18] T.F. Adepoju, M.A. Ibeh, E.N. Udoetuk, E.O. Babatunde, Quaternary blend of Carica papaya - Citrus sinesis - Hibiscus sabdariffa - waste used oil for biodiesel synthesis using CaO-based catalyst derived from binary mix of Lattorina littorea and Mactra coralline shell, Renew. Energy 171 (2021) 22–33.
[19] S. Sirisomboonchai, M. Abuduwayiti, G. Guan, C. Samart, S. Abliz, X. Hao, K. Kusakabe, A. Abudula, Biodiesel production from waste cooking oil using calcined scallop shell as catalyst, Energy Convers. Manag. 95 (2015) 242–247.
[20] J. Goli, O. Sahu, Development of heterogeneous alkali catalyst from waste chicken eggshell for biodiesel production, Renew. Energy 128 (2018) 142–154.
[21] Z.E. Tang, S. Lima, Y.L. Pang, H.C. Ong, K.T. Lee, Synthesis of biomass as heterogeneous catalyst for application in biodiesel production: state of the art and fundamental review, Renew. Sustain. Energy Rev. 92 (2018) 235–253.
[22] N. Asikin-Mijan, H.V. Lee, Y.H. Taufiq-Yap, Synthesis and catalytic activity of hydration–dehydration treated clamshell derived CaO for biodiesel production, Chem. Eng. Res. Des. 102 (2015) 368–377.
[23] W. Roschat, S. Phewphong, A. Thangthong, P. Moonsin, B. Yoosuk, T. Kaewpuang, V. Promarak, Catalytic performance enhancement of CaO by hydration-dehydration process for biodiesel production at room temperature, Energy Convers. Manag. 165 (2018) 1–7.
[24] N. Zhang, H. Xue, R. Hu, The activity and stability of CeO_2@CaO catalysts for the production of biodiesel, RSC Adv. 8 (2018) 32922–32929.
[25] S. Jairam, P. Kolar, R. Sharma-Shivappa, J.A. Osborne, J.P. Davis, KI-impregnated oyster shell as a solid catalyst for soybean oil transesterification, Bioresour. Technol. 104 (2012) 329–335.
[26] S.E. Mahesh, A. Ramanathan, K.M.M.S. Begum, A. Narayanan, Biodiesel production from waste cooking oil using KBr impregnated CaO as catalyst, Energy Convers. Manag. 91 (2015) 442–450.
[27] C. Komintarachat, S. Chuepeng, Catalytic enhancement of calcium oxide from green mussel shell by potassium chloride impregnation for waste cooking oil-based biodiesel production, Bioresour. Technol. Rep. 12 (2020), 100589.

[28] M.J. Borah, A. Das, V. Das, N. Bhuyan, D. Deka, Transesterification of waste cooking oil for biodiesel production catalyzed by Zn substituted waste egg shell derived CaO nanocatalyst, Fuel 242 (2019) 345–354.
[29] K.T. Tan, K.T. Lee, A.R. Mohamed, A glycerol-free process to produce biodiesel by supercritical methyl acetate technology: an optimization study via response surface methodology, Bioresour. Technol. 101 (2010) 965–969.
[30] B. Yoosuk, P. Udomsap, B. Puttasawat, P. Krasae, Modification of calcite by hydration–dehydration method for heterogeneous biodiesel production process: the effects of water on properties and activity, Chem. Eng. J. 162 (2010) 135–141.
[31] J. Huang, Y. Zou, M. Yaseen, H. Qu, R. He, Z. Tong, Fabrication of hollow cage-like CaO catalyst for the enhanced biodiesel production via transesterification of soybean oil and methanol, Fuel 290 (2021), 119799.
[32] S. Karnjanakom, A. Bayu, X. Hao, S. Kongparakul, C. Samart, A. Abudula, G. Guan, Selectively catalytic upgrading of bio-oil to aromatic hydrocarbons over Zn, Ce or Ni doped mesoporous rod-like alumina catalysts, J. Mol. Catal. A Chem. 421 (2016) 235–244.
[33] N. Mansir, S.H. Teo, N.A. Mijan, Y.H. Taufiq-Yap, Efficient reaction for biodiesel manufacturing using bi-functional oxide catalyst, Catal. Commun. 149 (2021), 106201.
[34] S. Palitsakun, K. Koonkuer, B. Topool, A. Seubsai, K. Sudsakorn, Transesterification of Jatropha oil to biodiesel using SrO catalysts modified with CaO from waste eggshell, Catal. Commun. 149 (2021), 106233.
[35] M.R. Abukhadra, A.S. Mohamed, A.M. El-Sherbeeny, A.T.A. Soliman, A.E.E. A. Elgawad, Sonication induced transesterification of castor oil into biodiesel in the presence of MgO/CaO nanorods as a novel basic catalyst: characterization and optimization, Chem. Eng. Process. Process. Intensif. 154 (2020), 108024.
[36] S. Karnjanakom, G. Guan, B. Asep, X. Hao, S. Kongparakul, C. Samart, A. Abudula, Catalytic upgrading of bio-oil over Cu/MCM-41 and Cu/KIT-6 prepared by β-cyclodextrin-assisted coimpregnation method, J. Phys. Chem. C 120 (2016) 3396–3407.
[37] R. Risso, P. Ferraz, S. Meireles, I. Fonseca, J. Vital, Highly active CaO catalysts from waste shells of egg, oyster and clam for biodiesel production, Appl. Catal. A 567 (2018) 56–64.
[38] W.U. Rahman, S.M. Yahya, Z.A. Khan, N.A. Khan, G. Halder, S.H. Dhawane, Valorization of waste chicken egg shells towards synthesis of heterogeneous catalyst for biodiesel production: optimization and statistical analysis, Environ. Technol. Innov. 22 (2021), 101460.
[39] M. Davoodbasha, A. Pugazhendhi, J.W. Kim, S.Y. Lee, T. Nooruddin, Biodiesel production through transesterification of Chlorella vulgaris: synthesis and characterization of CaO nanocatalyst, Fuel 300 (2021), 121018.
[40] H. Zhu, Z. Wu, Y. Che, P. Zhang, S. Duan, X. Liu, Z. Mao, Preparation of biodiesel catalyzed by solid super base of calcium oxide and its refining process, Chin. J. Catal. 27 (2006) 391–396.
[41] N. Viriya-empikul, P. Krasae, W. Nualpaeng, B. Yoosuk, K. Faungnawakij, Biodiesel production over Ca-based solid catalysts derived from industrial wastes, Fuel 92 (2012) 239–244.
[42] R. Foroutan, R. Mohammadi, J. Razeghi, B. Ramavandi, Biodiesel production from edible oils using algal biochar/CaO/K_2CO_3 as a heterogeneous and recyclable catalyst, Renew. Energy 168 (2021) 1207–1216.
[43] Y.S. Erchamo, T.T. Mamo, G.A. Workneh, Y.S. Mekonnen, Improved biodiesel production from waste cooking oil with mixed methanol–ethanol using enhanced eggshell-derived CaO nano-catalyst, Sci. Rep. 11 (2021) 6708.
[44] S. Karnjanakom, S. Kongparakul, C. Chaiya, P. Reubroycharoen, G. Guan, C. Samart, Biodiesel production from Hevea brasiliensis oil using SO_3H-MCM-41 catalyst, J. Environ. Chem. Eng. 4 (2016) 47–55.
[45] A. Piker, B. Tabah, N. Perkas, A. Gedanken, A green and low-cost room temperature biodiesel production method from waste oil using egg shells as catalyst, Fuel 182 (2016) 34–41.
[46] N. Widiarti, Y. La, N. mah, H. Bahruji, D. Prasetyoko, Development of CaO from natural calcite as a heterogeneous base catalyst in the formation of biodiesel: review, J. Renew. Mater. 7 (2019) 915–939.
[47] T. Roy, S. Sahani, D. Madhu, Y.C. Sharma, A clean approach of biodiesel production from waste cooking oil by using single phase $BaSnO_3$ as solid base catalyst: mechanism, kinetics & E-study, J. Clean. Prod. 265 (2020) (2020), 121440.
[48] Z. Zhu, Y. Liu, W. Cong, X. Zhao, J. Janaun, T. Wei, Z. Fang, Soybean biodiesel production using synergistic CaO/Ag nano catalyst: process optimization, kinetic study, and economic evaluation, Ind. Crops Prod. 166 (2021), 113479.
[49] D. Kumar, A. Ali, Nanocrystalline K-CaO for the transesterification of a variety of feedstocks: structure, kinetics and catalytic properties, Biomass Bioenergy 46 (2012) 459–468.
[50] M. Feyzi, L. Norouzi, Preparation and kinetic study of magnetic Ca/Fe_3O_4@SiO_2 nanocatalysts for biodiesel production, Renew. Energy 94 (2016) 579–586.
[51] K.N. Krishnamurthy, S.N. Sridhara, C.S.A. Kumar, Optimization and kinetic study of biodiesel production from *Hydnocarpus wightiana* oil and dairy waste scum using snail shell CaO nano catalyst, Renew. Energy 146 (2020) 280–296.
[52] L. Zhao, Z. Qiu, S.M. Stagg-Williams, Transesterification of canola oil catalyzed by nanopowder calcium oxide, Fuel Process. Technol. 114 (2013) 154–162.
[53] S.M. Pavlović, D.M. Marinković, M.D. Kostić, I.M. Janković-Častvan, L.V. Mojović, M.V.V. Stanković, V.B. Veljković, A CaO/zeolite-based catalyst obtained from waste chicken eggshell and coal fly ash for biodiesel production, Fuel 267 (2020), 117171.
[54] A. Naeem, I.W. Khan, M. Farooq, T. Mahmood, I.U. Din, Z.A. Ghazi, T. Saeed, Kinetic and optimization study of sustainable biodiesel production from waste cooking oil using novel heterogeneous solid base catalyst, Bioresour. Technol. 328 (2021), 124831.
[55] J. Calero, D. Luna, E.D. Sancho, C. Luna, E.M. Bautista, A.A. Romero, A. Posadillo, C. Verdugo, Development of a new biodiesel that integrates glycerol, by using CaO as heterogeneous catalyst, in the partial methanolysis of sunflower oil, Fuel 122 (2014) 94–102.
[56] L. León-Reina, A. Cabeza, J. Rius, P. Maireles-Torres, A.C. Alba-Rubio, M. L. Granados, Structural and surface study of calcium glyceroxide, an active phase for biodiesel production under heterogeneous catalysis, J. Catal. 300 (2013) 30–36.